Subinhibitory cefotaxime and levofloxacin contribute to selecting *Pseudomonas aeruginosa* from the coculture with *Staphylococcus aureus*

Kelei Zhao[1], Jing Li[1], Xiting Yang[1], Qianglin Zeng[2], Wei Liu[1], Yi Wu[1], Hui Zhou[2], Balakrishnan Prithiviraj[3], Xinrong Wang[1], Xikun Zhou[4,*], and Yiwen Chu[1,*]

[1] *Antibiotics Research and Re-evaluation Key Laboratory of Sichuan Province, School of Pharmacy, Chengdu University, Chengdu, Sichuan, China*

[2] *Department of Respiratory and Critical Care Medicine, Affiliated Hospital/Clinical College of Chengdu University, Chengdu, Sichuan, China*

[3] *Marine Bio-products Research Laboratory, Department of Plant, Food and Environmental Sciences, Dalhousie University, Truro, NS, Canada*

[4] *State Key Laboratory of Biotherapy and Cancer Center, West China Hospital, West China Medical School, Sichuan University, and Collaborative Innovation Center for Biotherapy, Chengdu, Sichuan, China.*

*For correspondence:

Xikun Zhou, State Key Laboratory of Biotherapy and Cancer Center, West China Hospital, Sichuan University and Collaborative Innovation Center for Biotherapy. No. 1, Keyuan 4th Road, Chengdu 610041, Sichuan, China. Tel.: +86-028-85367881. Email: xikunzhou@scu.edu.cn.

Yiwen Chu, School of Pharmacy, Chengdu University. No. 2025, Chengluo Avenue, Chengdu, 610106, Sichuan, China. Tel.: +86-028-84216035. Email: chuyiwen@cdu.edu.cn.

This file contains Supplementary Figures S1 to S13.

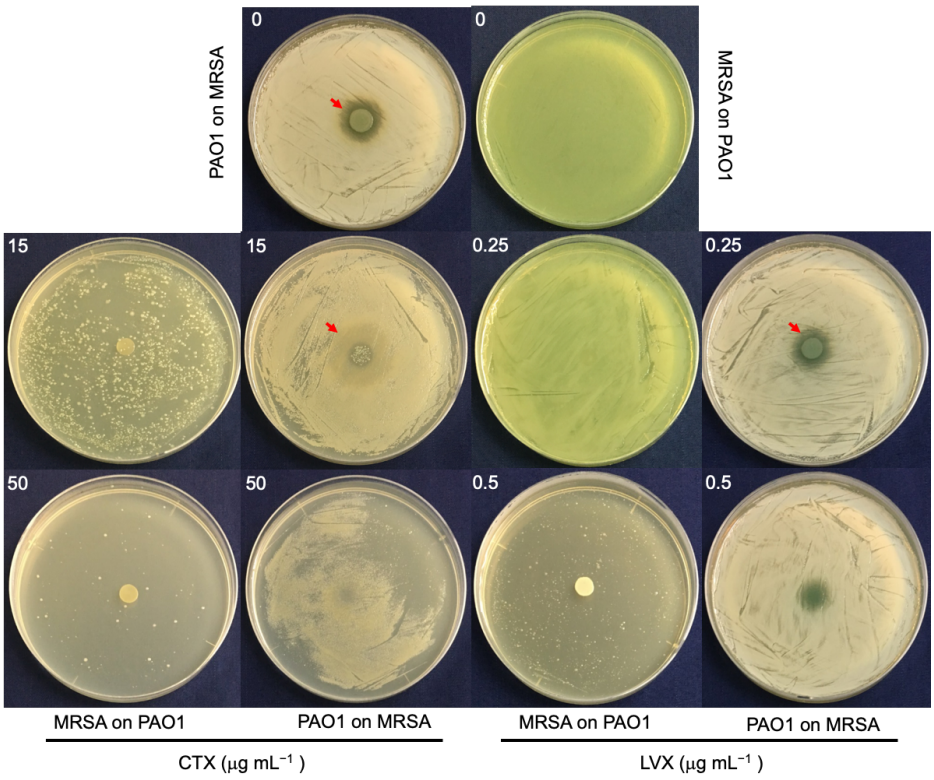

Fig. S1. Growth of *P. aeruginosa* PAO1 and *S. aureus* MRSA-COP112 on the lawn of each other on LB plates supplemented with different concentrations of cefotaxime and levofloxacin. Equal amount of PA- PAO1 and MRSA-COP112 were spotted on the lawn of each other and cultured for 24 h. Images are representative of three independent replicates. Dish size, 9 cm in diameter. Red arrow indicates the edge of inhibitory zone. CTX, cefotaxime. LVX, levofloxacin.

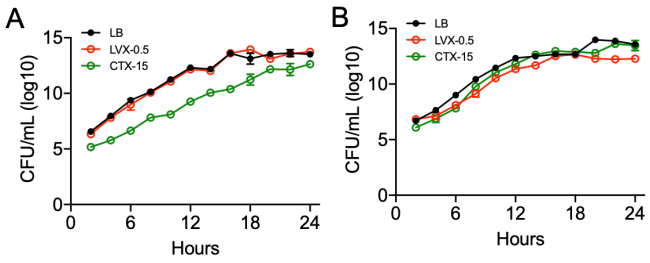

Fig. S2. Growth curves of MRSA-COP112 (A) and PA-COP2 (B) on LB plates containing 15 μg mL^{-1} of CTX or 0.5 μg mL^{-1} of LVX. Data shown are the means ± standard deviation (SD) of three independent replicates.

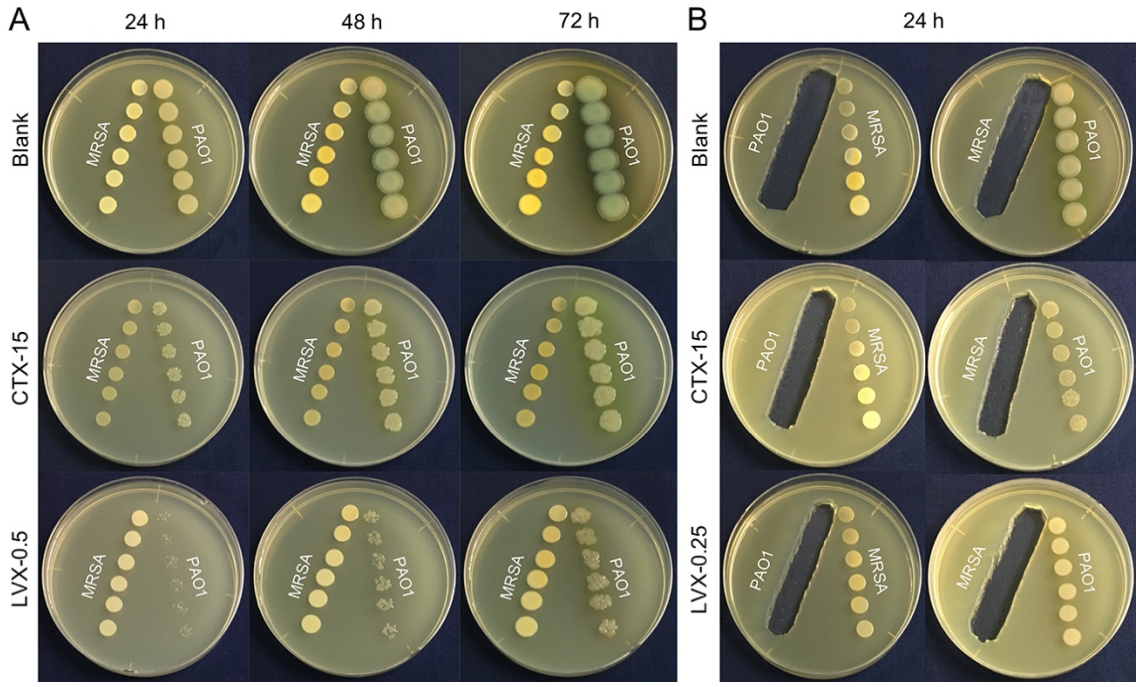

Fig. S3. Pairwise proximity assay of PA-PAO1 and MRSA-COP112. (A) Pairwise growth of PA-PA1 and MRSA-COP112 on LB plate containing subinhibitory CTX (15 μg ml^{-1}) or LVX (0.5 μg ml^{-1}) for different time durations. (B) Proximity of PA-PAO1 and MRSA-COP112 to the extracellular products of each other on LB plate containing subinhibitory CTX (15 μg ml^{-1}) or LVX (0.25 μg ml^{-1}) for 24 h. Images are representative of three independent replicates. Dish size, 9 cm in diameter.

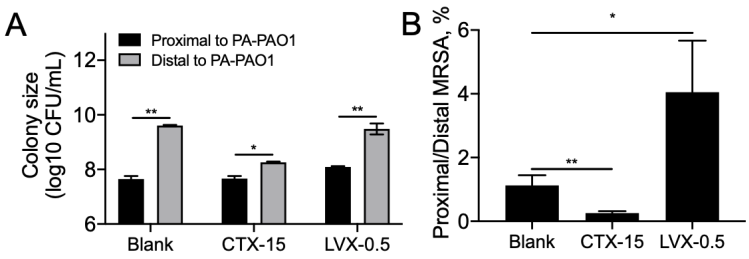

Fig. S4. Influences of CTX and LVX on the growth inhibition of MRSA-COP112 by the extracellular products of PA-PAO1. A. Colony sizes of MRSA-COP112 proximal and distal to the extracellular products of PA-PAO1 on blank LB and LB plates containing 15 μg mL^{-1} of CTX or 0.25 μg mL^{-1} of LVX. B. The colony sizes of MRSA-COP2 at the proximal ends were normalized (proximal CFUs/distal CFUs × 100%) to those at the distal ends on the same plates (corresponding to Fig. S3B). Data shown are the means ± SD of three independent replicates and compared by using two-tailed paired (A) and un-paired (B) *t*-test. *, $p < 0.05$. **, $p < 0.01$.

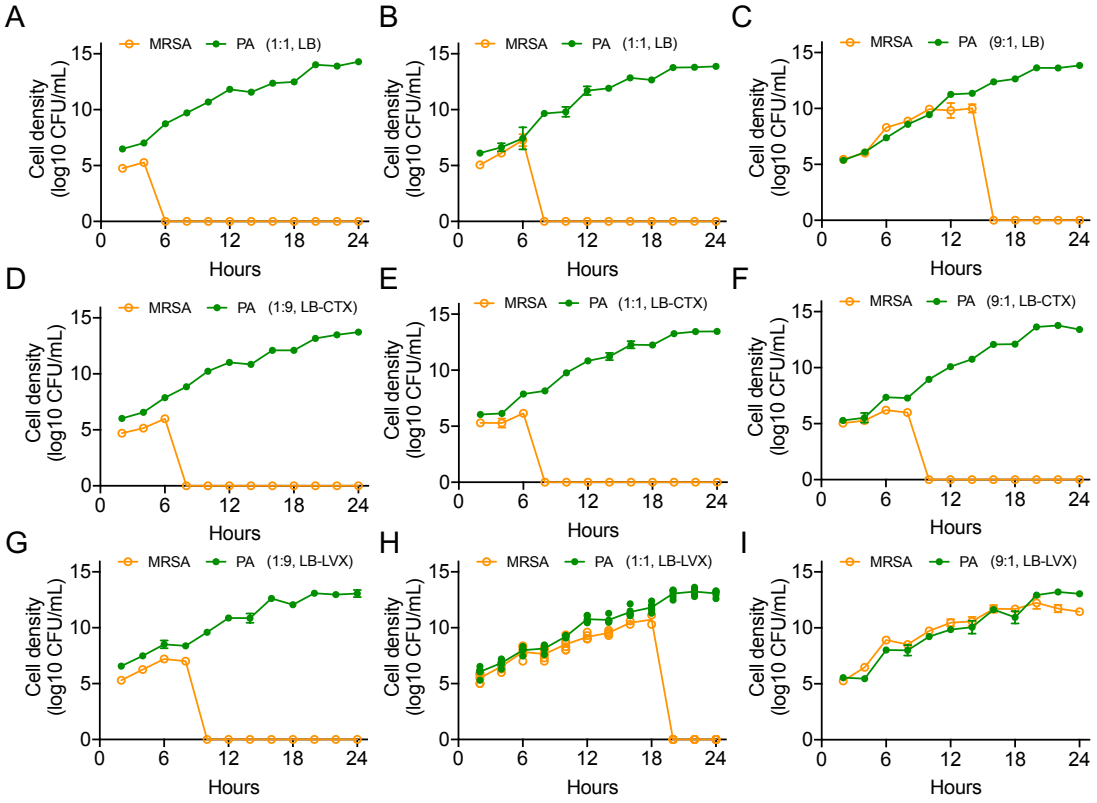

Fig. S5. Growth curves of PA-COP2 and MRSA-COP112 in the coculture. On-plate competition of PA-COP2 and MRSA-COP112 on (A-C) blank LB plates and LB plates containing subinhibitory (D-F) CTX and (G-I) LVX. Equal amount of PA-COP2 and MRSA-COP112 were mixed into the ratios of (A, D, G) 9:1, (B, E, H) 1:1, and (C, F, I) 1:9 and cocultured for different time durations. Bacterial cells from each time point were harvested for CFU enumeration and cell discrimination on blank LB and King's B plates. Data shown are the means ± SD of six independent replicates.

A

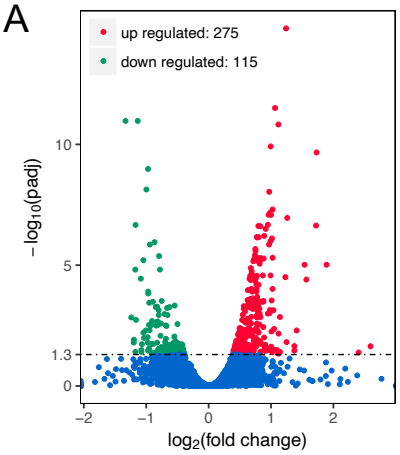

B

KEGG Terms	Gene No.	*p*-Value
Up-regulated		
Ribosome	13 (68)	0.00069141
Citrate cycle (TCA cycle)	7 (33)	0.00739815
Starch and sucrose metabolism	5 (18)	0.00905823
Carbon metabolism	14 (128)	0.03527835
Fructose and mannose metabolism	4 (19)	0.04122517
Down-regulated		
Sulfur metabolism	3 (51)	0.01678454
Oxidative phosphorylation	3 (55)	0.0203018
beta-Lactam resistance	2 (27)	0.0341739
Ribosome	3 (68)	0.0343362
ABC transporters	5 (193)	0.04814222

C

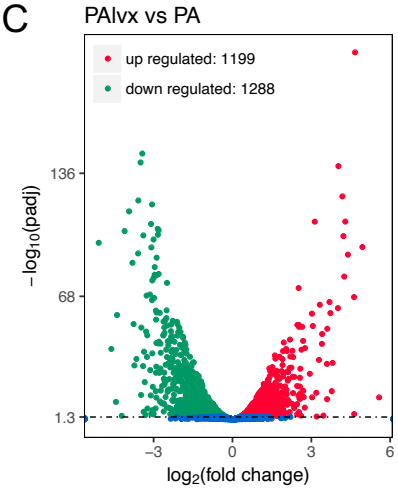

D

KEGG Terms	Gene No.	*p*-Value
Up-regulated		
Sulfur metabolism	33 (51)	1.57E-05
Purine metabolism	32 (77)	0.00715107
Riboflavin metabolism	7 (9)	0.02211784
RNA degradation	9 (15)	0.02920854
Down-regulated		
Valine, leucine and isoleucine degradation	23 (47)	0.00217222
Bacterial chemotaxis	21 (45)	0.00509275
Starch and sucrose metabolism	11 (18)	0.00961679
Biosynthesis of siderophore group nonribosomal peptides	6 (7)	0.01910044
Propanoate metabolism	19 (47)	0.02275123
Synthesis and degradation of ketone bodies	7 (10)	0.02302644
Tryptophan metabolism	12 (27)	0.03917916

Fig. S6. Influence of subinhibitory CTX and LVX on the transcriptional pattern of mono-cultured PA-COP2. Bacterial cells of PA-COP2 cultured on LB-CTX (15 μg mL^{-1}) and LB-LVX (0.5 μg mL^{-1}) plate were harvested at 24 h time point and conducted for RNA-sequencing. (A, C) Volcano plots and (B, D) significantly enriched KEGG terms by the differentially expressed genes in PA-COP2 cultured on (A, B) LB-CTX and (C, D) LB-LVX plate compared to that cultured on blank LB plate.

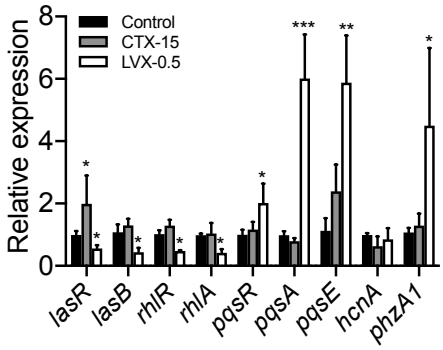

Fig. S7. Influence of subinhibitory CTX and LVX on the expression of typic QS-controlled genes as determined by quantitative PCR. Data shown are the means ± SD of three independent replicates and compared by using two-tailed un-paired *t*-test. *, $p < 0.05$. **, $p < 0.01$. ***, $p < 0.001$.

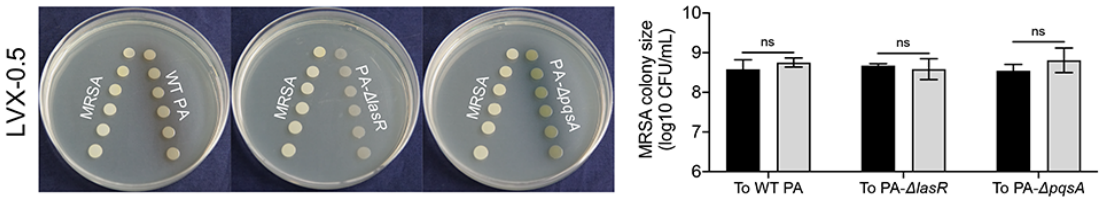

Fig. S8. Pairwise growth of MRSA-COP112 and PA-COP2 mutant strains on LB-LVX (0.5 μg mL^{-1}) plates for 24 h. Images are representative of three independent replicates. Data shown are the means ± SD of three independent replicates and compared by using two-tailed paired *t*-test. ns, Not significant.

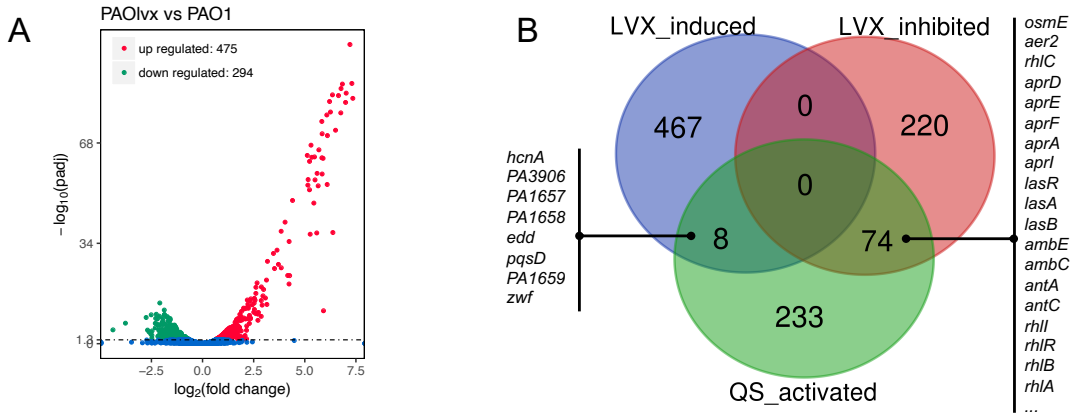

Fig. S9. Influence of subinhibitory LVX (0.25 μg mL^{-1}) on the transcriptional pattern of mono-cultured PAO1. (A) Volcano plots and (B) expression of QS-activated genes by the differentially expressed genes in PAO1 cultured on LB-LVX plate compared to that cultured on blank LB plate.

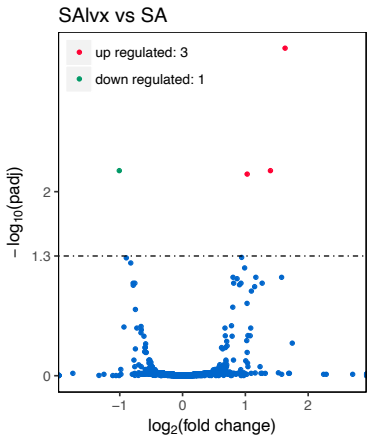

Fig. S10. Volcano plots by the differentially expressed genes in MRSA-COP112 cultured on LB-LVX plate compared to that cultured on blank LB plate.

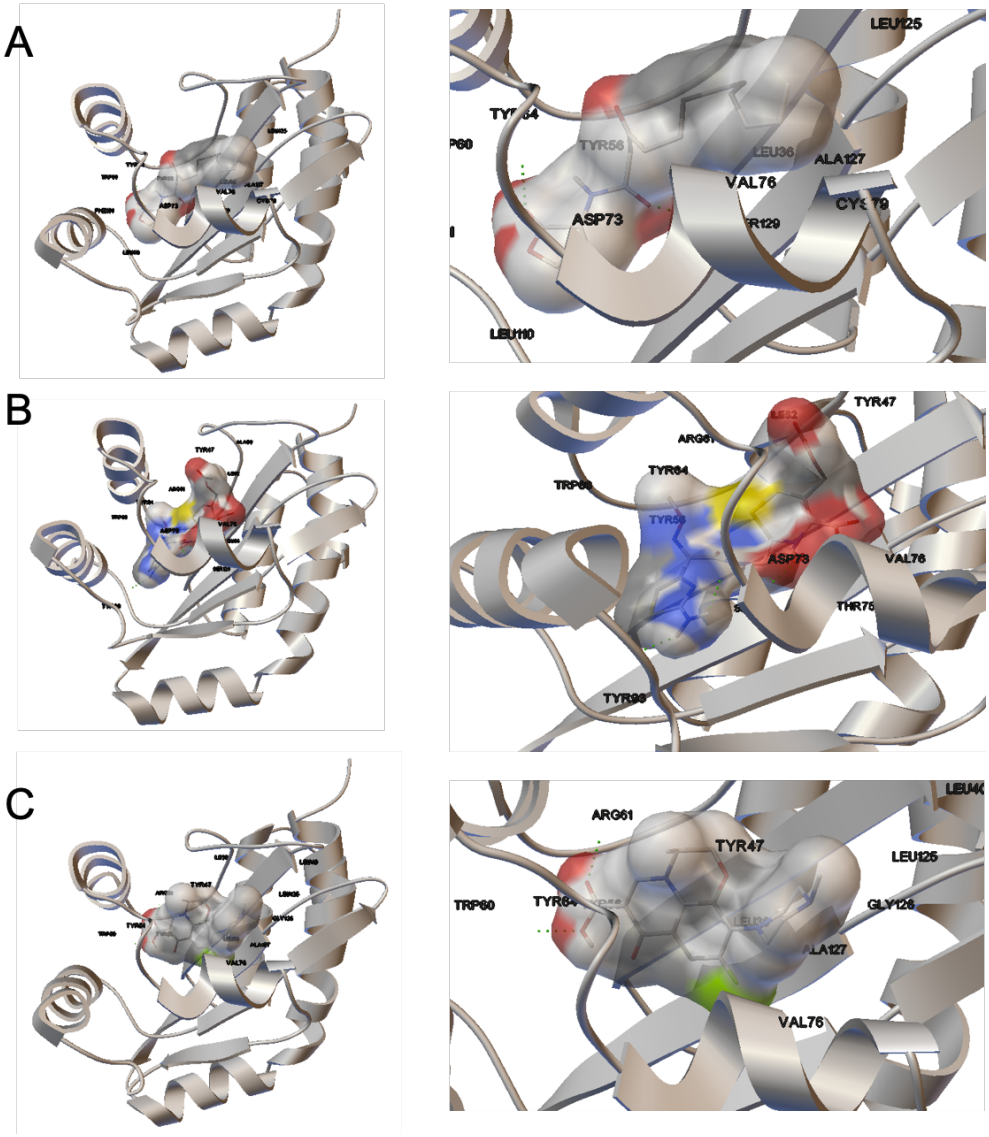

Fig. S11. Molecular docking of (A) native 3-oxo-C12-HSL signal, (B) CTX, and (C) LVX to LasR protein of *P. aeruginosa*. Panel A shows the binding of the native 3-oxo-C12-HSL signal to Trp-60 and Ser-129 of LasR with a Gibbs free energy (ΔG) of -7.65. Additionally, 3-oxo-C12-HSL can also bind to Thr-75 and Ser-129 with a ΔG of -7.28, bind to Tyr-56 and Ser-129 with a ΔG of -6.71, and bind to Arg-61 and Ser-129 with a ΔG of -6.64. Panel B shows the binding of CTX to Thr-75 of LasR with a ΔG of -9.08. CTX can also bind to Tyr-56 with a ΔG of -9.02, and to Trp-60 and Arg-61 with a ΔG of -8.98. Panel C shows the binding to LVX to Trp-60 and Arg-61 of LasR with ΔG ranged from -8.28 to -8.23. Aliphatic carbons in the ligand are gray-colored. Aromatic carbons in the ligand are green-colored. Nitrogens in the ligand are blue-colored. Oxygens in the ligand are red-colored. Sulfurs in the ligand are yellow-colored. The same below.

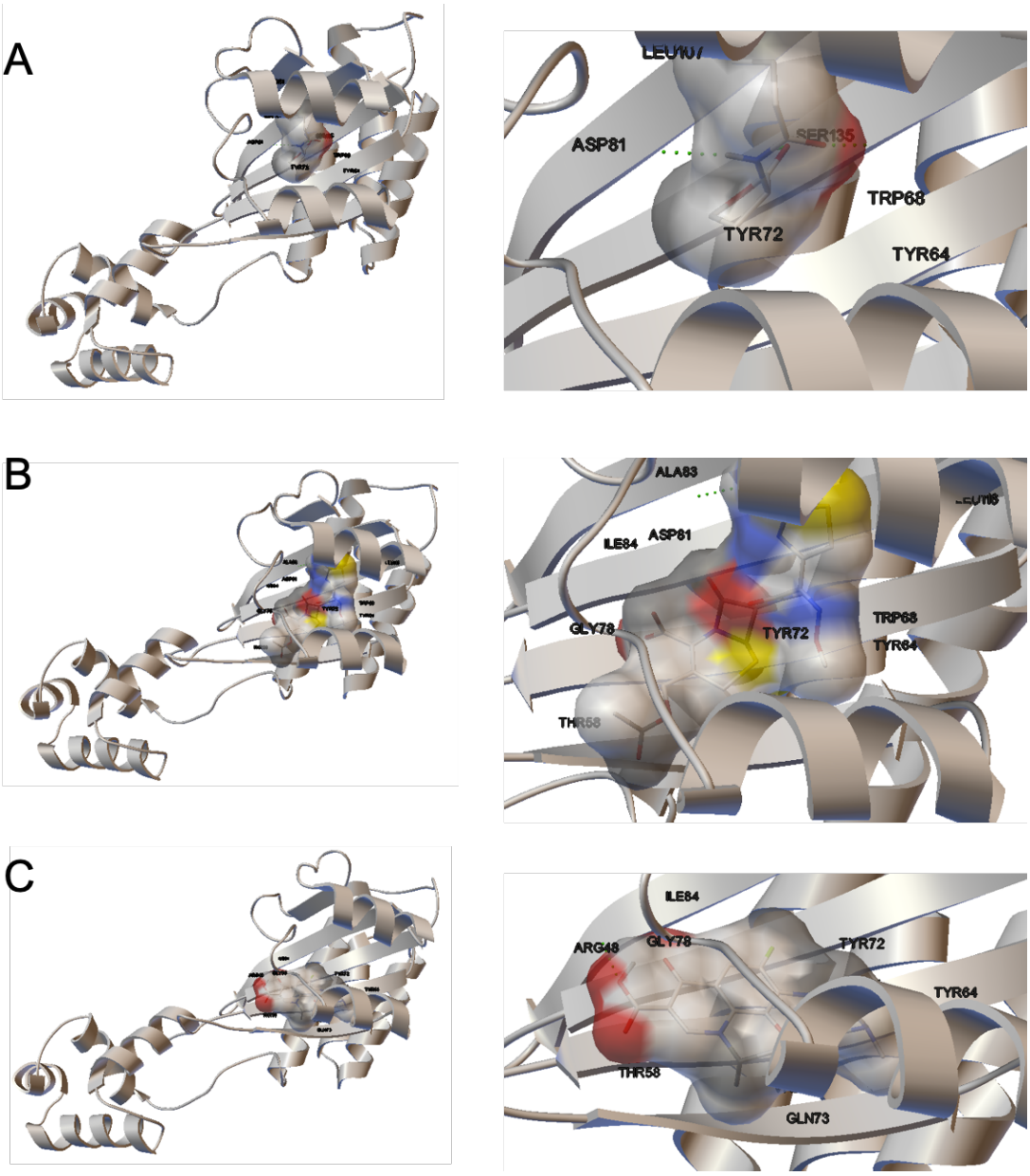

Fig. S12. Molecular docking of (A) native C4-HSL signal, (B) CTX, and (C) LVX to RhlR protein of *P. aeruginosa*. Panel A shows the binding of the native C4-HSL signal to Tyr-64 and Ser-135 of RhlR with a ΔG of -5.55. Additionally, C4-HSL can also bind to Tyr-72 and Ser-135 with a ΔG of -5.37. In panels B and C, although CTX and LVX can dock in the similar position to the ligand binding domain of RhlR with lower ΔG (-6.94 and -6.82, respectively) than the native C4-HSL signal, they failed to bind to any active sites of RhlR.

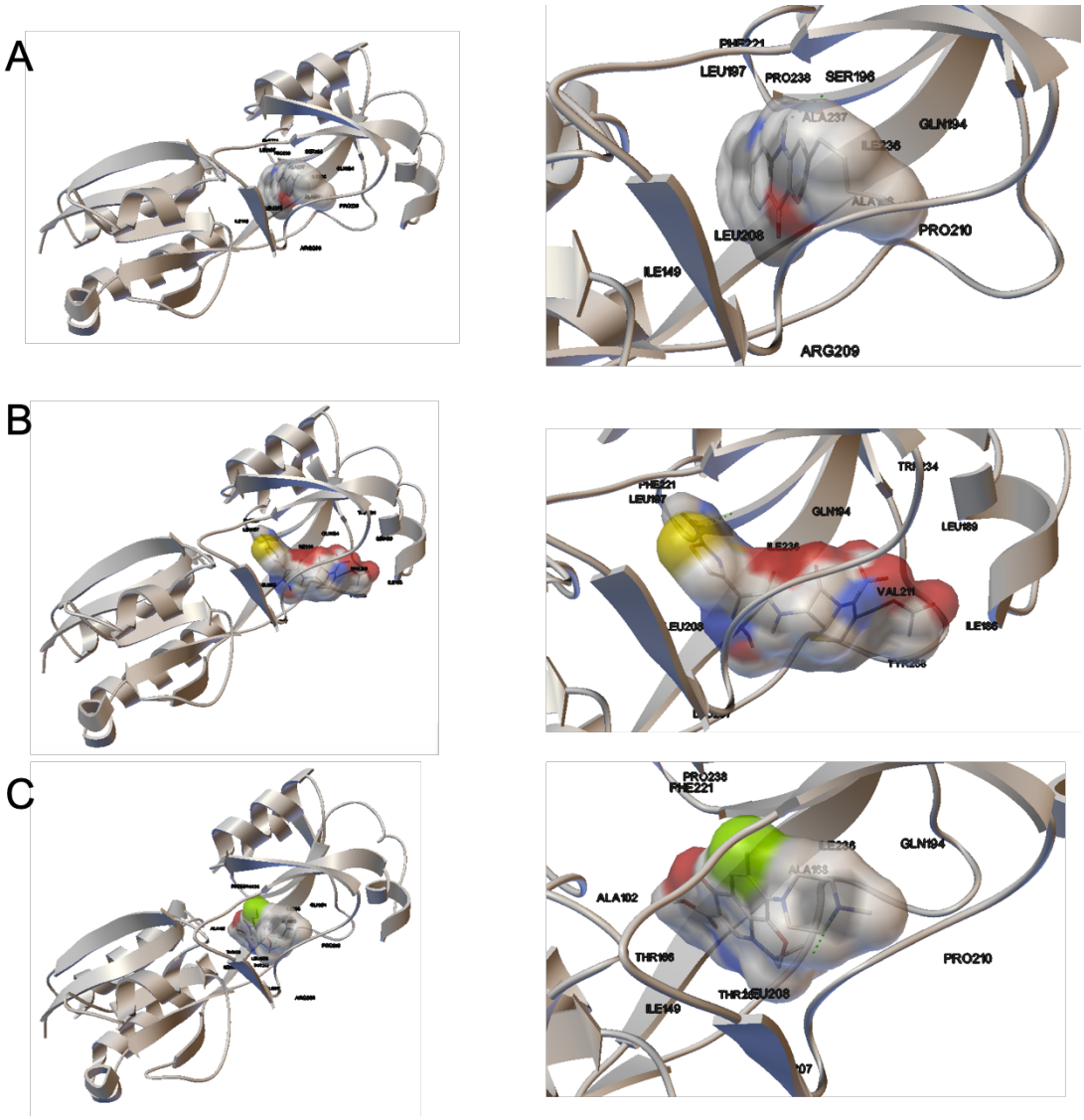

Fig. S13. Molecular docking of (A) native PQS signal, (B) CTX, and (C) LVX to PqsR protein of *P. aeruginosa*. Panel A shows the binding of the native PQS signal to Ser-196 of PqsR with a ΔG of -8.04. Panel B shows the possible binding of CTX to the ligand binding region (but not the active site) of PqsR with a ΔG of -4.51. In panel C, LVX can bind to the ligand binding region (but not the active site) of PqsR with a ΔG of -8.28, and the position of LVX in the pocket is similar to that of the native PQS signal.

Supplementary Datasets

Supplementary Dataset S1. Differentially expressed genes of PA-COP2 induced by CTX.

Supplementary Dataset S2. Differentially expressed genes of PA-COP2 induced by LVX.

Supplementary Dataset S3. Differentially expressed genes of PAO1 induced by LVX.

Supplementary Dataset S4. Differentially expressed genes of PA-COP2 on LB-LVX plate induced by the presence of MRSA lawn.

Supplementary Dataset S5. Differentially expressed genes of MRSA-COP112 on LB-LVX plate induced by the presence of PA-COP2 lawn.